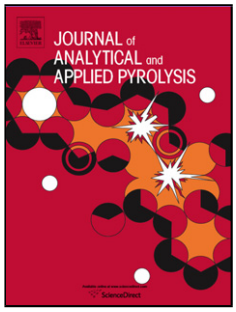

Title: Microstructural Characterization of White Charcoal

Author: C.H. Chia S.D. Joseph A. Rawal R. Linser J.M. Hook P. Munroe

PII: S0165-2370(14)00150-8
DOI: http://dx.doi.org/doi:10.1016/j.jaap.2014.06.009
Reference: JAAP 3226

To appear in: *J. Anal. Appl. Pyrolysis*

Received date: 29-1-2014
Revised date: 30-5-2014
Accepted date: 20-6-2014

Please cite this article as: C.H. Chia, S.D. Joseph, A. Rawal, R. Linser, J.M. Hook, P. Munroe, Microstructural Characterization of White Charcoal, *Journal of Analytical and Applied Pyrolysis* (2014), http://dx.doi.org/10.1016/j.jaap.2014.06.009

Microstructural Characterization of White Charcoal

C. H. Chia[a, *], S. D. Joseph[a], A. Rawal[b], R. Linser[b], J. M. Hook[b], P. Munroe[a]

[a]School of Materials Science and Engineering, University of New South Wales, Sydney, NSW 2052, Australia.

[b]Mark Wainwright Analytical Centre, University of New South Wales, Sydney, NSW, 2052, Australia

*Corresponding author: E-Mail: c.chia@unsw.edu.au

Tel.: + 61 2 9385 4435; Fax: + 61 2 9385 6400

Abstract - There has been an upsurge of interest in using high density and low volatile matter charcoal to replace coke and coal in the manufacture of aluminium and steel due to its potential to reduce net greenhouse gas emissions from the production process. 'White' charcoal is envisaged as a potential candidate for this application. It is synthesized by pyrolysing wood at low temperature (~240ºC) for 120 hours, and then raising the kiln temperature to ~1000ºC towards the end of the carbonization process. The charcoal is then withdrawn and smothered with a moistened mixture of earth, sand and ash. However, to date, little is known about the structure of this form of charcoal, which is essential before this material can be widely applied in extractive metallurgy. Characterization of white charcoal with nuclear magnetic resonance and x-ray photoelectron spectroscopy revealed a high fixed carbon content (>95 wt%) with ~82 at.% of the carbon present in the form of condensed aromatic rings. Scanning electron microscope

analysis depicts a porous microstructure with pores ~100 μm in diameter aligned across the surface and a high density of macropores <10 μm in diameter scattered across the surface. Transmission electron microscope and x-ray diffraction analysis of white charcoal showed a mainly amorphous carbon structure with localized regions of crystalline graphite and calcites. The suitability of white charcoal as a replacement for coke is also discussed.

Keywords : white charcoal; characterization; porosity; graphite

1. Introduction

'White' charcoal, also known as shiro-zumi or binchotan, is a traditional material widely used, especially in Japan, in a range of applications including in food preparation, as a smoke-free barbeque fuel. It is synthesized by pyrolysing hard woods, such as oak, at a relatively low temperature (~200-400 ºC) for a period, typically of a few days, and then raising the kiln temperature to ~1000 ºC towards the end of the pyrolysis process [1]. The white-hot charcoal is then withdrawn and smothered with a moistened mixture of earth, sand and ash. The term white charcoal arises from the use of ash to quench the material, which gives a pale grey hue to the charcoal surface. In addition to being used as fuel, products made from white charcoal including water purifiers, shampoos, and dehumidifiers are also readily available, especially in Japan. Some other applications of white charcoal include its use in radio frequency (RF) shielding [2], as an electromagnetic wave absorber [3-4], and as a bathroom deodorizer [5], which suggests that white charcoal has a range of novel properties.

Although widely used, almost nothing is known about the microstructure of white charcoal. Miao et al. [6] examined white charcoal particles using scanning electron microscopy (SEM), where it was shown that they exhibit a high density of pores, typically less than 10 μm in diameter, interspaced between larger pores typically around 50 μm in diameter. BET analysis of white charcoal by the same authors revealed a surface area of ~270 m^2/g. Miura [1] showed that white charcoal has a higher density and that the white charcoal that is carbonized from some wood feedstocks is denser than water. The measured densities of charcoal were found to reach a maximum at a final processing temperature of ~1000°C and it was deduced that the mechanisms involved in restructuring the carbonized wood at this temperature affect the morphology of the microstructure more than the morphology of the macrostructure [7]. The ignition point of white charcoal (300°C to 500°C) is also higher, and the yield of white charcoal is typically around 5% lower, compared with conventional black charcoals due to the final higher processing temperature employed. Miura [1] also found increasing the higher final temperature increased the hardness of the resultant white charcoal. White charcoal was also found to have a high adsorption capacity, where research has shown that gases such as ethylene [8], acetic acid vapour [9], and hydrogen [6] are strongly adsorbed by white charcoal. Wei et al. [10] found that white charcoal is strongly hydrophilic, whereas Hirokazu et al. [11] found that white charcoal is an effective additive to improve water quality through its high cation and anion leaching properties, as well as its high dissolved biochemical oxygen demand (BOD) adsorptive capacity. Even though white charcoal possesses many desirable properties, no detailed microstructural characterization of white charcoal has been carried out to the best of the authors' knowledge.

A number of countries are now looking at using high density and low volatile matter charcoal to replace coke and coal in the manufacture of aluminium and steel [12-13]. The main driver for the use of charcoal is the reduction in greenhouse gas emissions in the production process. Low density charcoal, with a relatively high volatile content, could potentially be used as a fuel in blast furnaces. For specialist applications, such as carburisation, the charcoal must have a higher density and a lower volatile content. As such, white charcoal is a potential option for this application. However, for white charcoal to find application in the steel industry, more detailed analysis of its physical and chemical properties is first required. The objective of this paper is, therefore, to present for the first time a detailed microstructural, chemical and spectroscopic characterization of white charcoal through a variety of methods, and to correlate the structure to both the processing conditions used and properties exhibited.

2. Materials and Methods

500g of white charcoal samples were obtained in the form of small logs (10 cm x 2 cm x 2 cm) supplied by Kemmy-Hi-Tek Ltd 175 Kamishiraki, Gyokuto-machi, Tamana-gun, Kumamoto Pref., Japan. Samples were crushed into millimeter-sized pieces prior to analysis. Various samples of these were used for analysis where possible. According to common procedures in charcoal analysis, representative mixtures from the set of samples were prepared where higher quantities are used only once (Nuclear magnetic resonance (NMR), X-ray photoelectron spectroscopy (XPS)). White charcoal is made in clay kilns whose height to length is maintain between 1:1 and 1:2. The chimney is at the back of the kiln on the floor and the door height is approximately ¾ of the maximum height of the kiln. Oak wood is stacked vertically in the kiln

and an external wood fire is ignited to slowly dry the oak and then to release the chemical water. The temperature of the wood is brought up to approximately 200°C and allowed to torrefy for a period of approximately 120 hours. The temperature is then increased to 600°C at 40°C/hr and then raised to approximately 1000°C at 50°C/minute. The charcoal is removed after 2 hours at 1000°C and quenched with a moist mixture of ash, clay, and sand. The kilns are run by experienced operators who very carefully control the rate of change in temperature and the white charcoal produced are sold internationally to a consistent standard and quality.

Ultimate and proximate analyses were performed by Bureau Veritas International Trade Pty Ltd in Australia using the relevant Australian standards (AS1038.3, AS1038.6.1 and AS1038.6.2). Density was measured using the water displacement method. XPS analysis was performed on a Thermo Scientific ESCALAB250Xi using a 500μm diameter beam of monochromatic Al-Kα radiation (photon energy = 1486.6 eV) at a pass energy of 20 eV. The core level binding energies (BEs) were aligned with respect to the C1s BE of 284.8 eV. X-ray diffraction (XRD) was carried out using a Philips X'pert Pro Multipurpose X-ray Diffraction System. A Cu source was used where the wavelength of $K\alpha^1$ is 0.15406 nm and the wavelength of $K\alpha^2$ is 0.15444 nm. A continuous scan was carried out with the scan range covering 2θ values from 10° to 90°. BET (Brunauer–Emmet–Teller) surface area were measured using a Micromeritics Tristar 3000 nitrogen adsorption apparatus at 77 K. The white charcoal particles were degassed under vacuum in a Micrometric VacPrep unit at 250°C overnight prior to surface area analysis to remove adsorbed water and volatile organics on the surface.

Solid-state NMR spectra were acquired using a Bruker Avance III-300 spectrometer operating at 75.39 MHz, and 299.77 MHz for ^{13}C and ^{1}H respectively, with a Bruker 4-mm double air-bearing cross-polarisation (CP) magic angle spinning (MAS) probe. To ensure representative analysis, finely ground, equal portions of several white charcoal samples (ca. 50 mg) were packed into 4-mm outside diameter zirconia rotors, and spun at 10 kHz MAS, the maximum allowed by the sample itself. These samples were highly conducting, which made normal data acquisition with ^{1}H decoupling very challenging, so caution needed to be applied. The ^{13}C spectra were acquired with 5 s recycle delay and with a single pulse, direct detection without decoupling, or with a Hahn echo (-90°-delay-180°-) and high-power SPINAL-64 ^{1}H decoupling on during the echo. ^{1}H decoupling was achieved with the SPINAL-64 sequence having an effective field strength of ~50 kHz used in specific experiments. Approximately 12-20 k scans were acquired for sufficient signal/noise. The free induction decays were processed with zero-filling to 8 K prior to Fourier transformation with Gaussian broadening. Chemical shifts were referenced to the carbonyl peak of solid glycine at δ_C 176 ppm, and this sample was also used to set up the Hartmann-Hahn matching for CP. For the labeled benzene experiment, [U-13C]-benzene (5 mg, 99 atom%, Cambridge Isotopes, USA) was added to the white charcoal, and then packed into the 4 mm rotor, for data acquisition.

Scanning electron microscope (SEM) analysis of the microstructure of white charcoal was performed using a Hitachi S3400 SEM. Analysis of approximately ten white charcoal pieces was carried out to determine the range of particle types and their nominal composition. Approximately fifteen different white charcoal pieces (based on size and physical characteristics) were then mounted in epoxy resin and polished using methods described by Chia et al. [14].

Distinctive phases were identified and elemental analysis was then carried out on polished cross-sections using a JEOL JXA-8500F Field-Emission SEM-EPMA (electron probe micro-analyzer). Transmission electron microscope (TEM) samples were prepared by pulverizing the charcoal and dispersing the powder in ethanol and pipetting droplets onto a holey carbon 3mm copper grid. The samples were then examined using a Philips CM 200 TEM to which energy dispersive X-ray spectroscopy (EDS) facilities were attached. To ensure representative analysis more than ten pieces were examined using both SEM and TEM due to the relatively heterogeneous nature of the charcoal particles. However, the observations made across the particles examined were found to be broadly consistent and the micrographs shown in this paper are representative of the areas examined.

3. Results and Discussions

Proximate analysis of white charcoal (Table 1) showed the material to be >95% (by mass) fixed carbon with an ash content of 2.1% and low volatile matter content, which is broadly similar to prior studies of commercially available white charcoal carbonized from oak wood [15]. The fixed carbon content was found to be similar to the fixed carbon content of olive stones carbonized at 1000°C and much higher compared to other biomass, such as tree cuttings and grape vines, carbonized at a similar temperature [16], which suggest that besides that final carbonizing temperature, the raw materials used may determine the final fixed carbon content.

The high fixed carbon content of white charcoal could be attributed to the low ash content of the oak wood used as a feedstock. The low volatiles content of white charcoal indicates that it is difficult to ignite due to the lack of readily combustible low molecular weight compounds and that it burns very cleanly [16], consistent with the reported properties of white charcoal by one of its commercial manufacturers [17]. The wood is torrefied at 240°C and the long steaming time at low temperatures (~200°C) slowly degrades the lignocellulosic structure of the biomass and results in a charcoal that probably has different chemical and physical properties to those produced at higher heating rates and temperatures [18]. The prolonged heating time at low temperatures will cause the white charcoal to have higher water absorption and broadened pore size distribution due to the slowly degrading lignocellulosic structure of the wood [19]. The long heating time can also lead to deacetylation, and the acetic acid released can act as a depolymerization agent and promote the decomposition of polysaccharide [20]. The high temperatures used while producing white charcoal are also reflected in the low H/C (0.061) and O/C (0.026) ratios. The H/C ratio of less than 0.1 suggests that white charcoal has a graphite-like structure [21]. The density of the white charcoal was measured to be 1.27 g/cm^3, which is higher than the density measured by Miura [1]. The BET surface area was measured to be 0.183 m²/g, which is lower compared to the value reported by Rajkovich et al. [22] for non-activated oak biochars synthesised at 600 °C. This could be due to the higher HTT used for the production of white charcoal, which could cause the collapse of the pores and thus result in a lower surface area.

The XPS wide scan spectrum for white charcoal is shown in Fig. 1a and the deconvolution of the carbon 1s peak is shown in Fig. 1b. The carbon 1s peak was deconvoluted into four different

peaks [23-24], where binding energies of 285.0 eV, 286.2 eV, 287.2 eV and 288.4 eV, correspond to C-C/C=C, C-O-C, C=O and a π -π* shake up feature respectively. The graphitic (C=C) and the aliphatic (C-C) are fitted together into one peak due to the close proximity of their binding energy [25]. Table 2 shows that white charcoal has a total carbon content of ~93 at.% with ~82 at.% of the carbon present in the form of condensed aromatic rings and aliphatic groups. Very few oxygenated functional groups were detected by XPS, which is consistent with the findings of the proximate and ultimate analysis and again suggest that white charcoal is chemically stable. The low concentration of oxygen atoms that remained even after carbonizing at 1000°C are involved in the cross-linking of the carbon microstructure, which produces a non-graphitizing hard carbon [26]. The π -π* shake up satellite peak at ~290 eV can be attributed to the effect of polycondensed carbon cluster development that leads to the formation of a delocalized π electron system [27]. Nishimiya et al. [24] showed that the peak width of the C1s spectrum gets sharper, whereas the intensity of the O1s peak decreases, as the carbonization temperature increases. The structural characteristics deduced from the XPS studies are supported by measurements using ^{13}C solid-state NMR spectroscopy as discussed below.

White charcoal displays a high degree of conductivity that makes solid-state NMR spectroscopy of the material very challenging. The influence of this conductivity is two-fold. Firstly, the quality factor of the probe, which is the direct measure of how efficiently electrical power is converted into the radio frequency pulses necessary for NMR, is significantly affected. In the current case, the quality factor of the probe deteriorated to the point that high power ^{1}H decoupling during acquisition could not always be safely performed. Secondly, the conductive nature of the white charcoal limits the ability to spin the NMR rotor at maximum speed in the

magnetic field. In this instance by limiting the sample volume to only half the 4 mm rotor, a MAS speed of 10 kHz was achievable (as opposed to a limit of 14 kHz for non-conducting material). The directly-polarized ^{13}C NMR spectrum of the white charcoal shows that the carbon is almost exclusively aromatic without a detectable presence of aliphatic carbon species. The aromatic carbon signal is a single broad peak resonating with a chemical shift of δ_C of 115 ppm (Fig. 2a) and a Full Width at the peak Half Maximum (FWHM) of 50 ppm. Compared to δ_C 128.7 ppm ^{13}C chemical shift of benzene, the carbon species of the white charcoal resonate at a significantly shielded lower ppm. This reduction in the chemical shift of the white charcoal can be explained by the formation of larger clusters of fused aromatic rings during the carbonization process. In such large clusters, the aromatic ring current exerts a strong shielding influence, which causes the carbons to resonate at a lower ppm. Fig. 2b shows the directly polarized ^{13}C spin-echo MAS NMR spectrum of the white charcoal, which shows the central peak shifted to δ_C 122 ppm. This difference in the chemical shift between the single-pulse and spin echo experiments (Fig. 2a and Fig. 2b respectively) is not immediately clear. However, it is hypothesized that the carbon species resonating at lower ppm may have a shorter transverse relaxation time than the carbon species resonating at a higher ppm. Thus, the spin-echo experiment would be selective towards the carbon species with the longer relaxation times. The origin of the differential ^{13}C transverse relaxation among the carbon species may correspond to their site specific location, for example towards the edge of a condensed aromatic cluster versus the middle of the cluster.

An auxiliary method to measure the degree of aromatic condensation of a char, as suggested by Smernik et al. [28], was also employed. About 5 mg of uniformly ^{13}C-labeled benzene was adsorbed onto the white charcoal and the resulting ^{13}C NMR spectrum was measured (Fig. 2c). The chemical shift of the adsorbed benzene, δ_C 119 ppm, yields a -9.7 ppm ($\Delta\delta$) chemical shift relative to neat benzene. This approximately -10 ppm value for ($\Delta\delta$) is consistent with the production of biochar at temperatures of about 1000 ^oC [29], similar to those of biochars from coconut husks, red gum wood and phalaris straw, synthesized by pyrolysis at temperatures of 850°C or above [30].

Fig. 3 shows a series of SEM images acquired from a white charcoal particle. A low magnification secondary electron image (Fig. 3a) reveals the coarse structure of the white charcoal particle. Numerous pores ~100 μm in diameter appear aligned across the particle surface, which is consistent with the structure observed by Miao et al. [6]. A higher magnification secondary electron image of the same particle is shown in Fig. 3b. It can be seen that in addition to the large macropores shown in Fig. 3a, the surface of white charcoal contains a high density of smaller macropores <10 μm in diameter. That is, there is a bimodal distribution of pores. A backscattered electron image taken from a polished cross-section (Fig. 3c) shows a microstructure containing pores of various sizes, some of which are filled with the quenching ash used in the production process. The macropores are again aligned. Fig. 3d shows a higher magnification backscattered electron image of the white charcoal's surface, where the quenching materials appear to fill up most, but not all, of the larger sized pores.

A series of elemental X-ray maps were recorded, using a microprobe, from a white charcoal particle around an ash particle embedded in one of the pores in the white charcoal (Fig. 4). The wavelength dispersive X-ray spectroscopy (WDS) elemental maps reveal that the ash particle is most probably a calcium oxide particle due to its high Ca and O content. A small number of particles that are rich in Si, Al, and O were also found scattered randomly within the pores and are likely to be clay particles. Examination of the Al map showed a low concentration of this element distributed across the entire sample, which confirms that the quenching materials consist of both aluminium oxides and clay particles. In addition, particles that are rich in Ca and P show that the quenching ash also contains some calcium phosphate particles.

TEM analysis shows the microstructure of this material at a higher spatial resolution. Fig. 5a shows a bright field image of a white charcoal particle together with the surrounding quenching ash aggregate at relatively low magnification. The carbon-rich regions, for example on the right hand side of fig. 5a, marked X, exhibited little evidence of crystalline structure. A selected area diffraction pattern acquired from this region presents as a ring pattern consistent with an amorphous crystal structure (Fig. 5d). This is in contrast to the highly graphitized structures observed in charcoals prepared at temperatures in excess of 2000 °C [31]. Analysis of the regions containing the Ca-rich phases, marked Y (Fig. 5a), indicated a structure of nanoscale crystalline phases. A higher magnification image of this region is shown in Fig. 5b. Mixtures of nanocrystalline phase are found in close proximity to each other. Selected area diffraction patterns acquired from these regions (Fig. 5c), indicated the presence of the {012} plane (d-spacing = 2.68 Å), the {112} plane (d-spacing = 2.33Å), and the {132} plane (d-spacing = 1.80Å) of calcium carbonate. The {0002} plane of graphite (d-spacing = 3.66Å) was also detected. It

appears that these regions of the microstructure consist of an intimate mix of graphite and calcium-rich phases, typically a few 10's of nanometers in size.

X-ray diffraction analysis (Fig. 6) shows a broad peak at 25°, which can be indexed as the (0002) plane of graphite. The smaller peaks at 43° and 54° are assigned to the {1010}/{1011} and {0004} planes of graphite respectively [32]. The weak diffraction is expected for non-graphitizable carbonized cellulosics [7] and the broader peaks at 25° and 43° that were obtained are consistent with the presence of amorphous carbon and/or the presence of nanoparticles. The peak around 29° is characteristic of the (104) plane of calcite, which is part of the quenching materials used.

Characterization of white charcoal reveals a microstructure similar to turbostratic carbon that is different from other charcoals carbonized at similar temperatures due to its unique processing conditions. Even though the final carbonizing temperature of white charcoal is relatively high (~1000 °C) compared with conventional charcoal manufacturing standards (~500 °C), no long range ordered structure such as an onion-like graphitic structure [33] or any ordered graphite planes were observed. This might be due to the lack of catalyst elements such as Fe, Co, or Ni, which will lower the temperature needed for graphitization [34]. In the absence of the aforementioned catalytic elements, graphitization tends to occur at temperatures of 1800°C and above. The XRD analysis results, which are consistent with the TEM results, were similar to the findings of Nishimiya et al. [23], where it was found that a sharp graphite peak only started to appear in charcoal carbonized at temperatures of 1800°C and above.

Drawing together the analysis of white charcoal from a range of methods reveals that it exhibits a high density, a low volatile matter content, together with a high percentage of fixed carbon and a low sulphur content. This suggests that it has the chemical and physical properties which make it a potential replacement for coke and coal in the primary processing of aluminium and steel [12-13]. However, alternative methods of quenching white charcoal, such as water or air quenching, could be trialled to replace the traditional Japanese methods of quenching. This would be desirable to lower the final ash content of the white charcoal. An additional benefit of using white charcoal as a replacement for coke is the reduction in greenhouse gas emissions relative to current practice. The production cost of white charcoal is, however, higher compared to conventional coke. Nevertheless, white charcoal can be produced from renewable sources that may be specifically grown for the purposes of charcoal production. A research program has been initiated by an industry collaborator to determine if white charcoal can be produced at a lower cost using either invasive species of hardwood or waste timber that would normally be sent to landfill. This process will use the waste heat from adjacent carbonizing kilns to torrefy the hardwood for a long period of time before bringing it to carbonizing temperatures. These materials will then be tested to determine their suitability for use in either steel making or recarburisation.

4. Conclusion

In summary, white charcoal has a range of unique properties due to the processing conditions used in the traditional production methods. Detailed characterization of white charcoal through a

range of techniques revealed a deeper understanding of the structure of this material. It was shown that white charcoals has a high fixed carbon content (>95 wt%) with ~82 at.% of the carbon present in the form of condensed aromatic rings mixed with aliphatic groups, as confirmed by solid state ^{13}C NMR spectroscopy. Microscopy characterization revealed a porous microstructure containing a mixture of amorphous carbon structure with localized region of crystalline graphite and calcites. White charcoal can be a potential replacement to coke and coal due to its low volatile, high density, and low sulphur content.

References

[1] I. Miura, Manufacture of charcoal in Japan with special reference to its properties, Industrial and Engineering Chemistry 23 (1931) 631-34.

[2] H. Norikane, T. Nishikubo, S. Gokyu, K. Itoh, M. Itoh, RF magnetic shielding effects of a compound plate constructed from bincho-charcoal and ferrite plates, IEEE Transactions on Applied Superconductivity 16 (2006) 1765-68.

[3] H. Miki, T. Kukuchi, M. Nakamura, Development of electromagnetic wave absorber with white charcoal, Trans Mater Res Soc Jpn 29 (2004) 2443-46.

[4] Y. Uchida, M. Nakanishi, T. Fujii, J. Takada, A. Muto, Y. Sakata et al, Crystalline control of bincho charcoal by using catalytic graphitization and electromagnetic wave absorption characteristics of derived carbon, Trans Mater Res Soc Jpn 29 (2004) 2511-14.

[5] N. Kazue. Natural soap containing bincho-zumi powder. Japan patent 10-298595 A. 1998

[6] H.Y. Miao, G.R. Chen, D.Y. Chen, J.T. Lue, M.S. Yu, Hydrogen storage: a comparison of hydrogen uptake values in carbon nanotubes and modified charcoals, EPJ Appl. Phys. 52 (2010) 21101.

[7] C.E. Byrne, D.C. Nagle, Carbonized wood monoliths – characterization, Carbon 35 (1997) 267-273.

[8] J.M. Won, J.Y. Song, Development of inner packaging material for maintaining the freshness of fruits and vegetables, Journal of Korea Technical Association of the Pulp and Paper Industry 39 (2007) 64-68.

[9] A. Ikuo, I. Satoshi, M. Jun, F. Tomoko, Deodorization performance of charcoal, Science and Industry 74 (2000) 106-11.

[10] Y. Wei, L. Wu, C. Wang, Analysis of the factors affecting the hydrophobicity of composite insulator in atmosphere condition, High Voltage Engineering 32 (2006) 31-34.

[11] K. Hirokazu, Estimation of cation and anion leaching characteristics and dissolved BOD-adsorption capacity of homemade charcoal produced by community participation. Bulletin of Minamikyushu University, Natural Science 36 (2006) 7-20.

[12] J.G. Mathieson, H. Rogers, M.A. Somerville, S. Jahanshahi, Reducing net CO_2 emissions using charcoal as a blast furnace tuyere injectant, ISIJ International 52 (2012) 1489-96.

[13] T. Norgate, N. Haque, M. Somerville, S. Jahanshahi, Biomass as a source of renewable carbon for iron and steelmaking. ISIJ international 52 (2012) 1472-1481.

[14] C.H. Chia, P. Munroe, S. Joseph, Y. Lin, Microscopic characterisation of synthetic Terra Preta, Australian Journal of Soil Research 48 (2010) 593-605.

[15] J.L. Deenik, A. Diarra, G. Uehara, S. Campbell, Y. Sumiyoshi, M.J. Antal Jr, Charcoal ash and volatile matter effects on soil properties and plant growth in an acid ultisol, Soil Science 176 (2011) 336-45.

[16] T. Griessacher, J. Antrekowitsch, S. Steinlechner, Charcoal from agricultural residues as alternative reducing agent in metal recycling, Biomass and Bioenergy 39 (2012) 139-46.

[17] whitecharcoal.com [Internet]. [cited 2013 Jul 4]. Available from: http://whitecharcoal.com/index.php.

[18] FAO Forestry Department. Simple technologies for charcoal making. Rome Italy, Chapter 10, 1987

[19] S. Hietala, S.L. Maunu, F. Sundholm, S. Jamsa, P. Viitaniemi, Structure of thermally modified wood studied by liquid state NMR measurements, Holzforschung 56 (2002) 522-28.

[20] D. Fengel, On the changes of the wood and its components within the temperature range up to 200°C – part 2, Holz Roh-Werkst 24 (1966) 98-109.

[21] E. Krull, J. Baldock, J. Skjemstat, R. Smernik, Characteristic of biochar: Organo-chemical properties, In: J. Lehmann, S. Joseph (Eds.), Biochar for environmental management. Science and Technology, Earthscan, London, 2009, pp. 53-66.

[22] S. Rajkovich, A. Enders, K. Hanley, C. Hyland, A.R. Zimmerman, J. Lehmann, Corn growth and nitrogen nutrition after additions of biochars with varying properties to a temperate soil, Biol. Fertil. Soils 48 (2012) 271–284.

401 [23] Z.R. Yue, W. Jiang, L. Wang, S.D. Gardner, C.U. Pittman Jr, Surface characterization of
402 electrochemically oxidized carbon fibers, Carbon 37 (1999) 1785–96.

403

404 [24] K. Nishimiya, T. Hata, Y. Imamura, S. Ishihara, Analysis of chemical structure of wood
405 charcoal by X-ray photoelectron spectroscopy, Journal of Wood Science 44 (1998) 56-61.

406

407 [25] L.A. Langley, D.E. Villanueva, D.H. Fairbrother, Quantification of surface oxides on
408 carbonaceous materials, Chem Mater 18 (2005) 169–78.

409

410 [26] G.M. Jenkins, K. Kawamura, Polymeric carbons – carbon fibre, glass and char. Cambridge
411 University Press, Cambridge, 1976.

412

413 [27] Y.R. Rhim, D. Zhang, D.H. Fairbrother, K.A. Wepasnick, K.J. Livi, R.J. Bodnar et al.,
414 Changes in electrical and microstructural properties of microcrystalline cellulose as function of
415 carbonization temperature, Carbon 48 (2010) 1012-1024.

416

417 [28] R.J. Smernik, R.S. Kookana, J.O. Skjemstad, NMR characterization of ^{13}C-benzene sorbed
418 to natural and prepared charcoals, Environmental Science and Technology 40 (2006) 1764–1769.

419

[29] A.V. McBeath, R.J. Smernik, M.P.W. Schneider, M.W.I. Schmidt, E.L. Plant, Determination of the aromaticity and the degree of aromatic condensation of a thermosequence of wood charcoal using NMR, Organic Geochemistry 42 (2011) 1194–1202.

[30] A.V. McBeath, R.J. Smernik, Variation in the degree of aromatic condensation of chars, Organic Geochemistry 40 (2009) 1161-68.

[31] T. Hata, K. Yamane, E. Kobayashi, Y. Imamura, S. Ishihara, Microstructural investigation of wood charcoal made by spark plasma sintering, Journal of Wood Science 44 (1998) 332-34.

[32] Y. Kodama, K. Sato, K. Suzuku, Y. Saito, T. Suzuku, T. Konno, Electron microscope study of the formation of graphitic nanostructures in nickel-loaded wood char, Carbon 50 (2012) 3486-96.

[33] T. Hata, Y. Imamura, E. Kobayashi, K. Yamane, K. Kikuchi, Onion-like graphitic particles observed in wood charcoal, Journal of Wood Science 46 (2000) 89-92.

[34] T. Hata, Y. Imamura, K. Nishimiya, P. Bronsveld, T. Vystavel, J. De Hosson J et al, Electron microscopic study on catalytic carbonization of biomass carbon: I. carbonization of

439 wood charcoal at high temperature by Al-Triisopropoxide, Mol. Cryst. Liq. Cryst 386 (2002) 33-
440 38.

441

441 **Figure Captions**

442

443 **Fig. 1a** XPS wide scan showing the binding energy of O (~532 eV), Ca (~347 eV), C (~285 eV),
444 and Si (~102 eV). Fig. 1b. Narrow scan of C1s showing the deconvolution of the C1s peak

445

446 **Fig. 2a** Directly-polarized ^{13}C NMR spectrum of white charcoal, Fig. 2b shows the directly
447 polarized ^{13}C spin- echo NMR spectrum, Fig. 2c shows the ^{13}C labeled benzene adsorption
448 spectrum

449

450 **Fig. 3** SEM images acquired from a typical white charcoal particle. Fig. 3a is a low
451 magnification secondary electron image showing the rough structure of white charcoal. Fig. 3b
452 shows a high magnification secondary electron image of the white charcoal's surface. Fig. 3c is a
453 low magnification backscattered electron image of the polished cross-section of white charcoal.
454 Fig. 3d shows a backscattered electron image of the minerals used in the quenching process
455 filling up the pores of white charcoal

456

457 **Fig. 4** Elemental EDS maps showing a calcium-rich particle embedded in one of the white
458 charcoal's pores. Traces of P, Al, K, and Si are also found scattered randomly in the pores. The
459 concentration of the respective elements are represented on a nominal intensity spectrum from
460 red to purple with red being the highest concentration of the particular element.

461

462 **Fig. 5a** Bright field TEM image showing a carbon-rich region (X) and a calcium-rich region (Y),
463 b) close up of region Y showing the crystalline lattice structure c) selected area diffraction
464 pattern from region Y, d) selected area diffraction pattern from region X

465

466 **Fig. 6** XRD spectrum of white charcoal

467

Highlights

White charcoal was synthesized using traditional Japanese methods.

Characterization was performed by a range of microscopy and spectroscopy techniques.

A heavily porous structure with a high fixed C content was observed.

This material may potentially replace coke in steel processing

Table 1. Proximate analysis and ultimate analysis (dry basis) of white charcoal as provided by Bureau Veritas Pty. Ltd.

	% Ash	% Volatiles	% Fixed Carbon	% C	% H	% N	% S	% O	H/C	O/C
White charcoal	2.1	2.8	95.1	93.9	0.48	0.22	0.02	3.27	0.061	0.026

Table 2: XPS results for white charcoal, showing atomic% for all elements detected

	at%	Centre (eV)	Structure	at%
O 1s	6.2	531.2	O-C	6.2
N 1s	0.2	400.7		0.2
Ca $2p_{3/2}$	0.6	347.0		0.6
C 1s	92.8	285.0	C-C/C=C	82.4
		286.2	C-O-C	6.8
		287.2	C=O	2.9
		288.4	π -π*	0.6
Si 2p	0.2	102.3	silicates	0.2

Figure 1

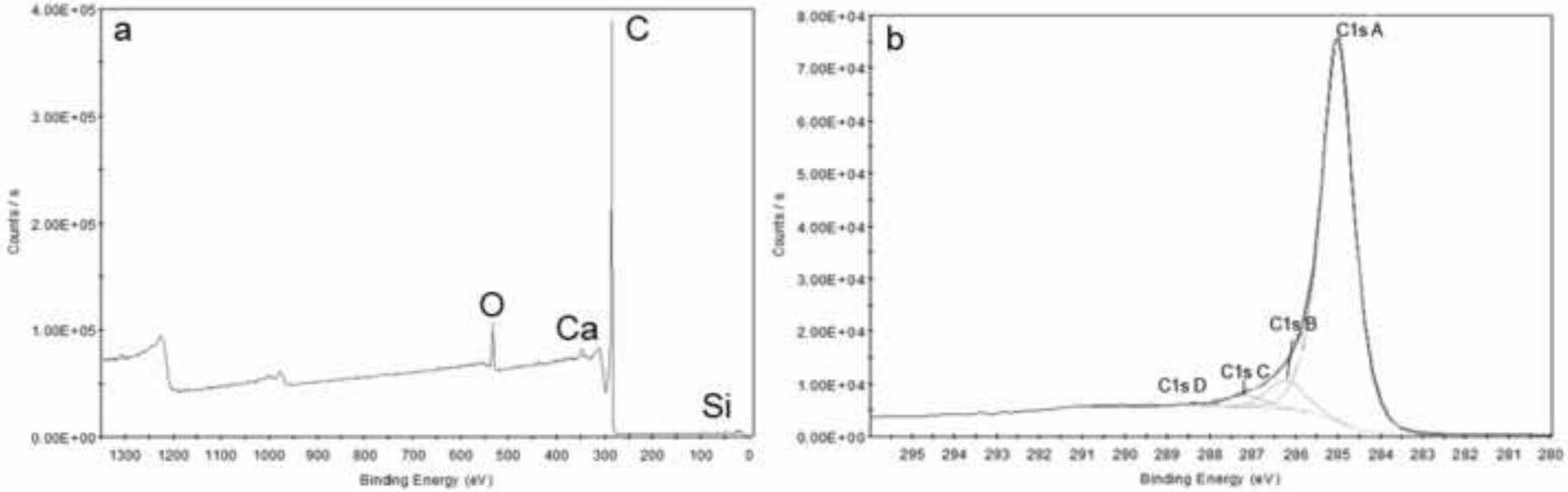

Figure 2

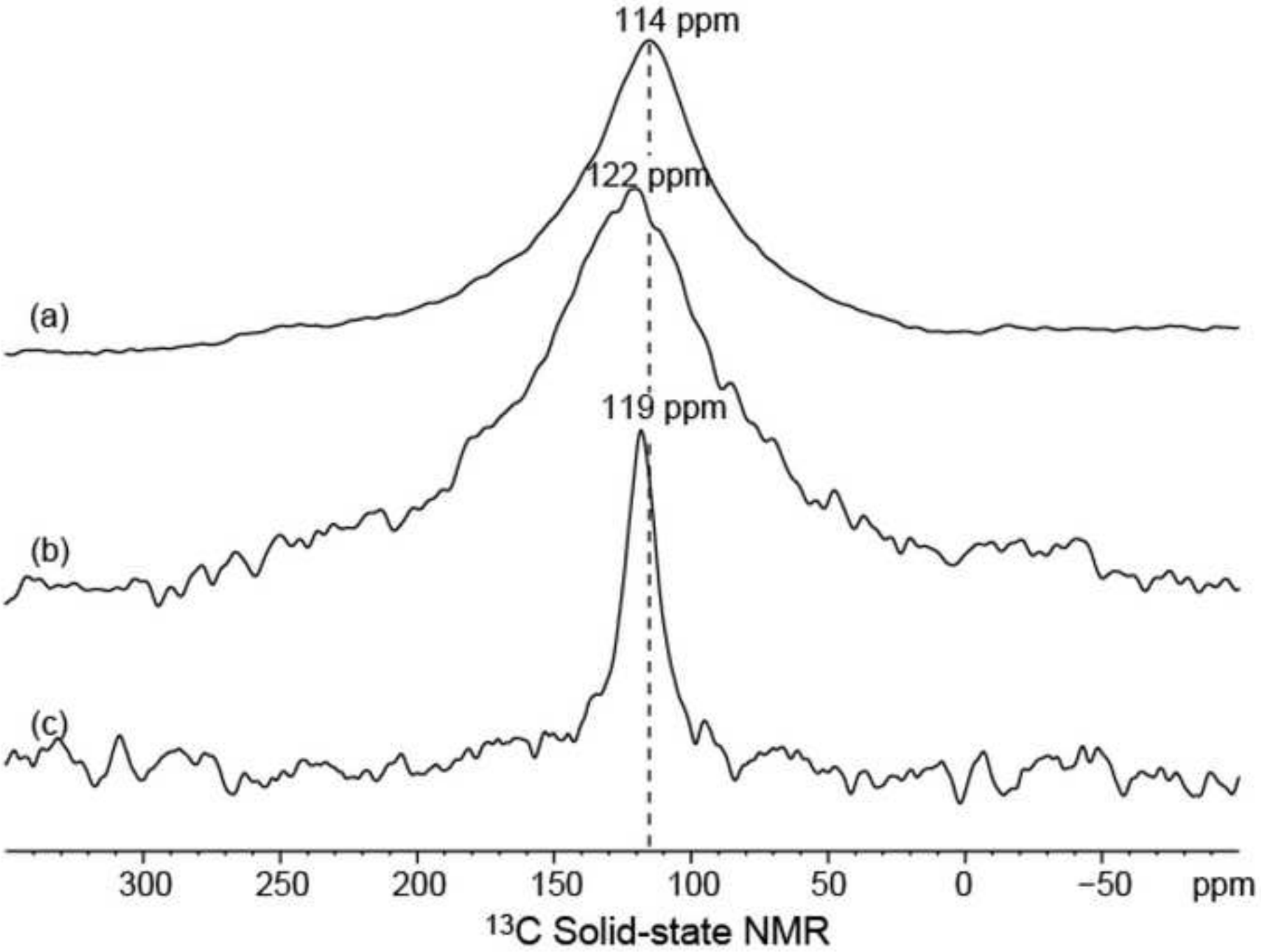
114 ppm
122 ppm
(a)
119 ppm
(b)
(c)
300
250
200
150
100
50
0
−50
ppm
13C Solid-state NMR

Figure 3

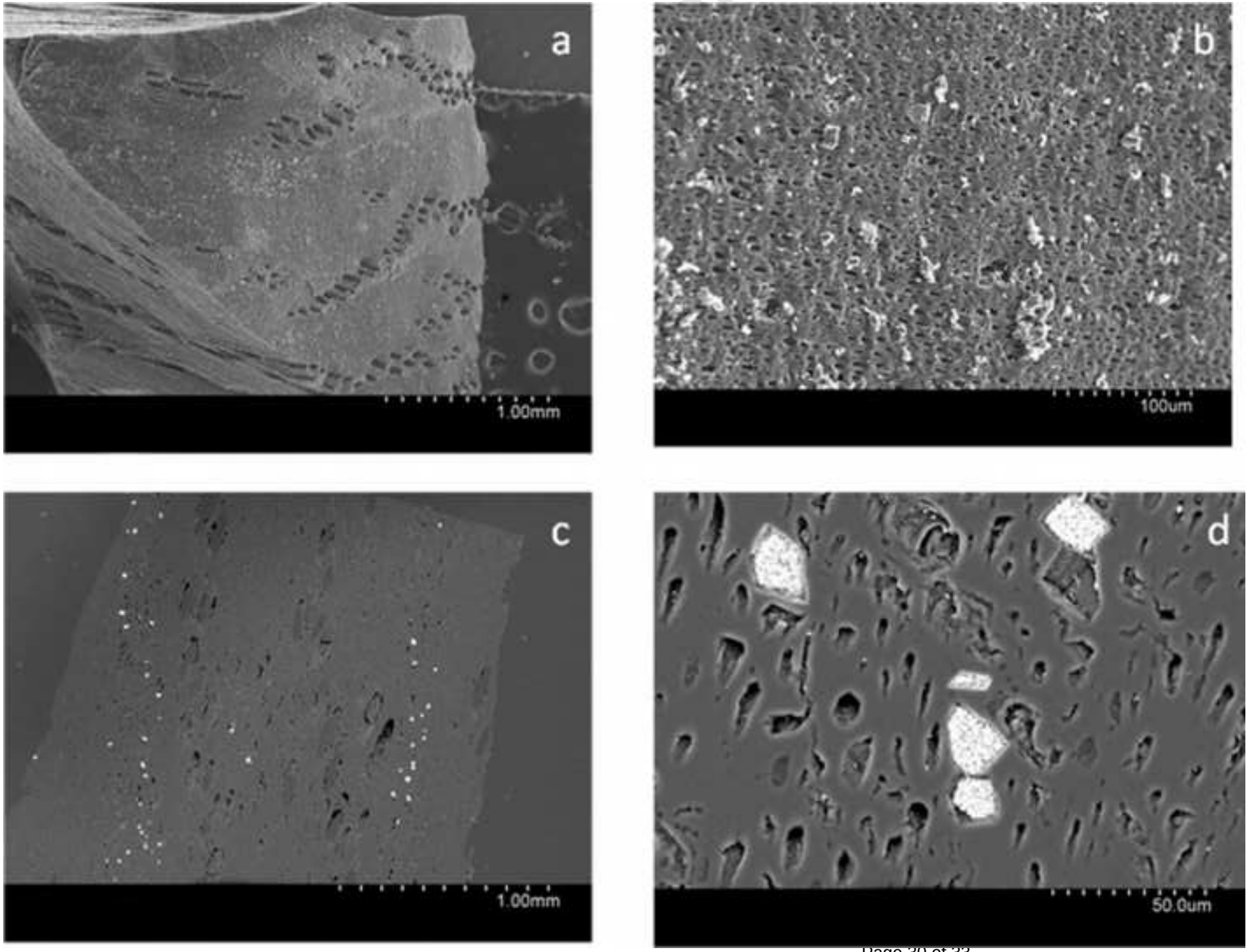

Figure 4

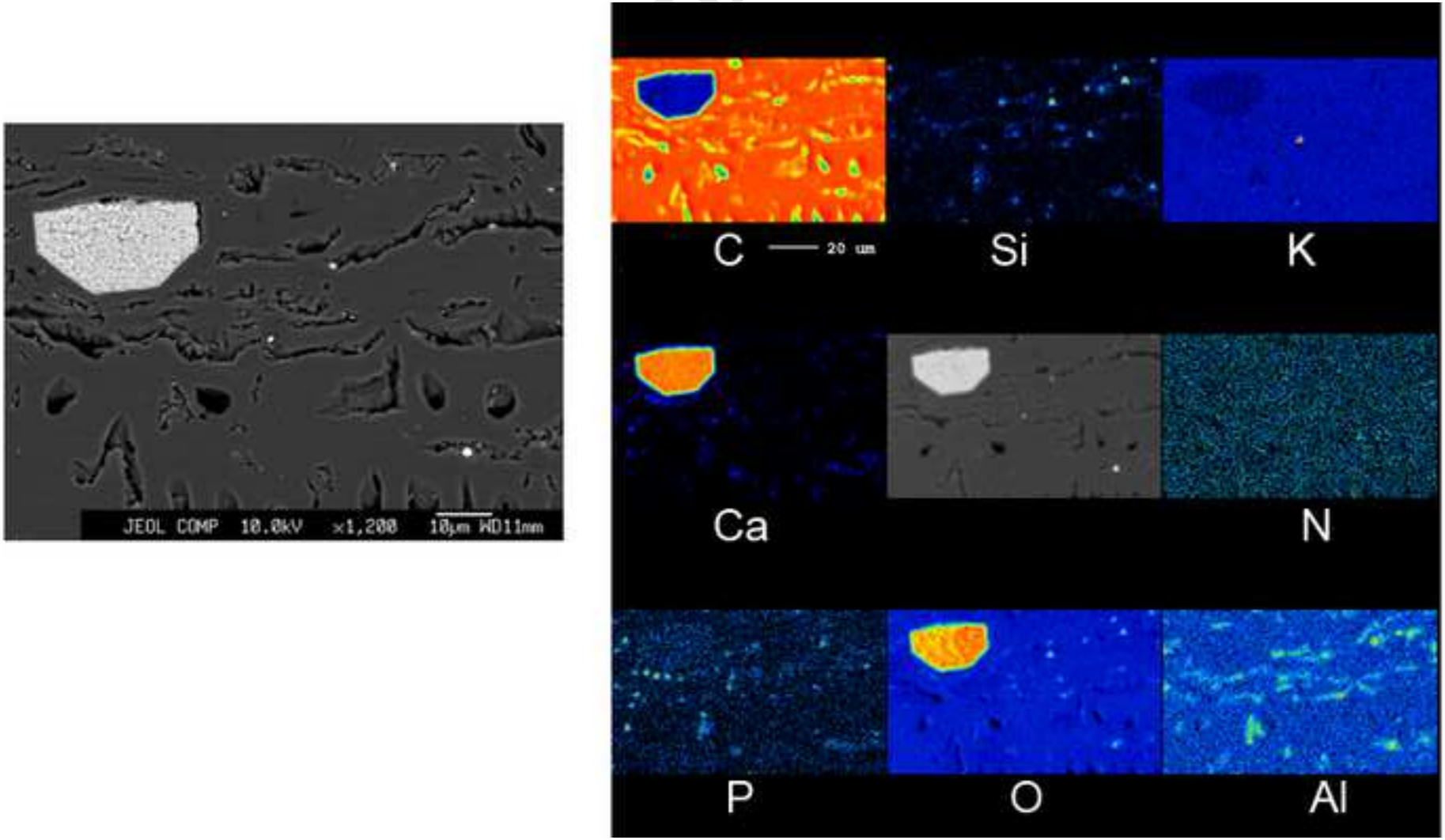

Figure 5

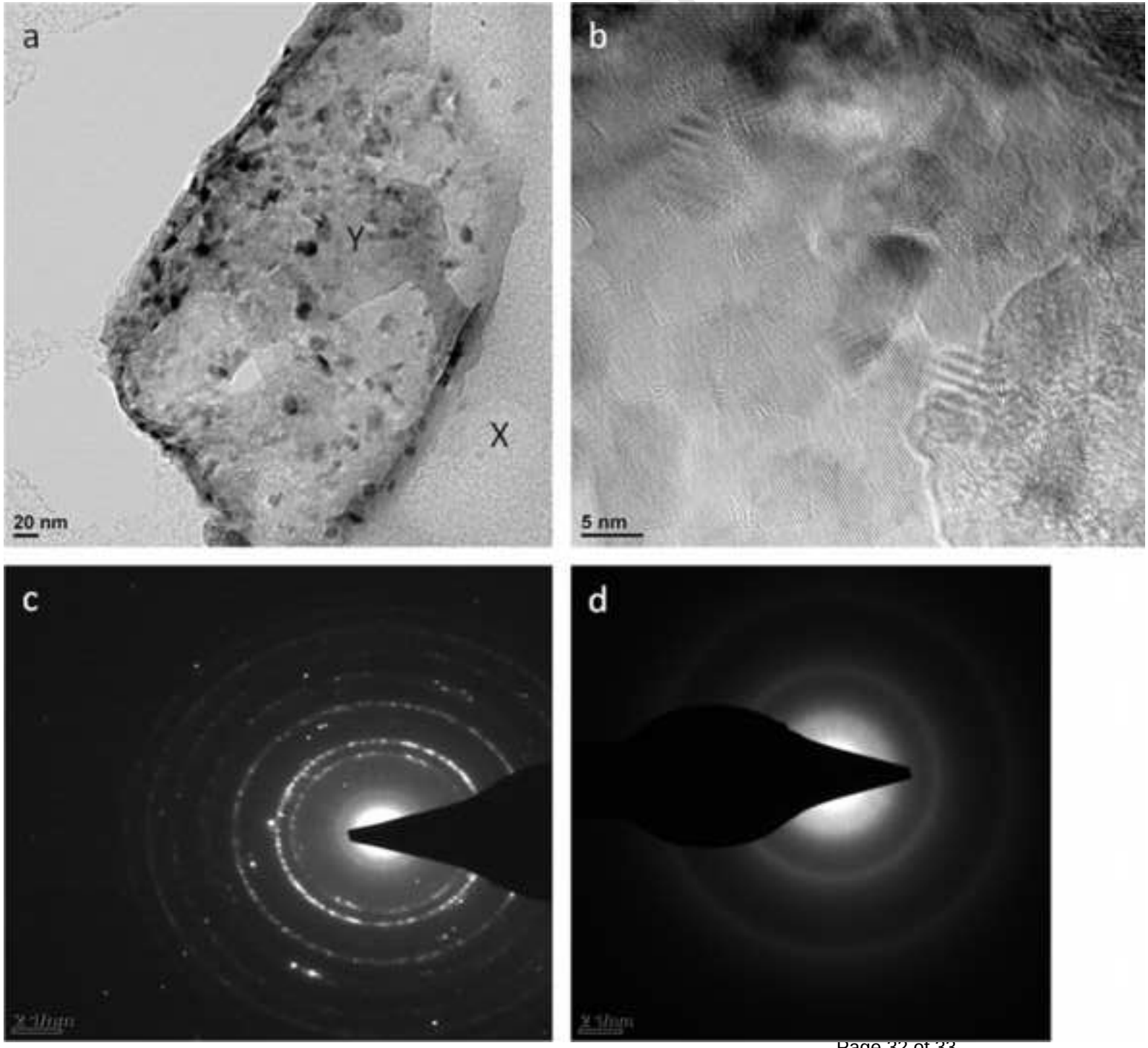

Figure 6

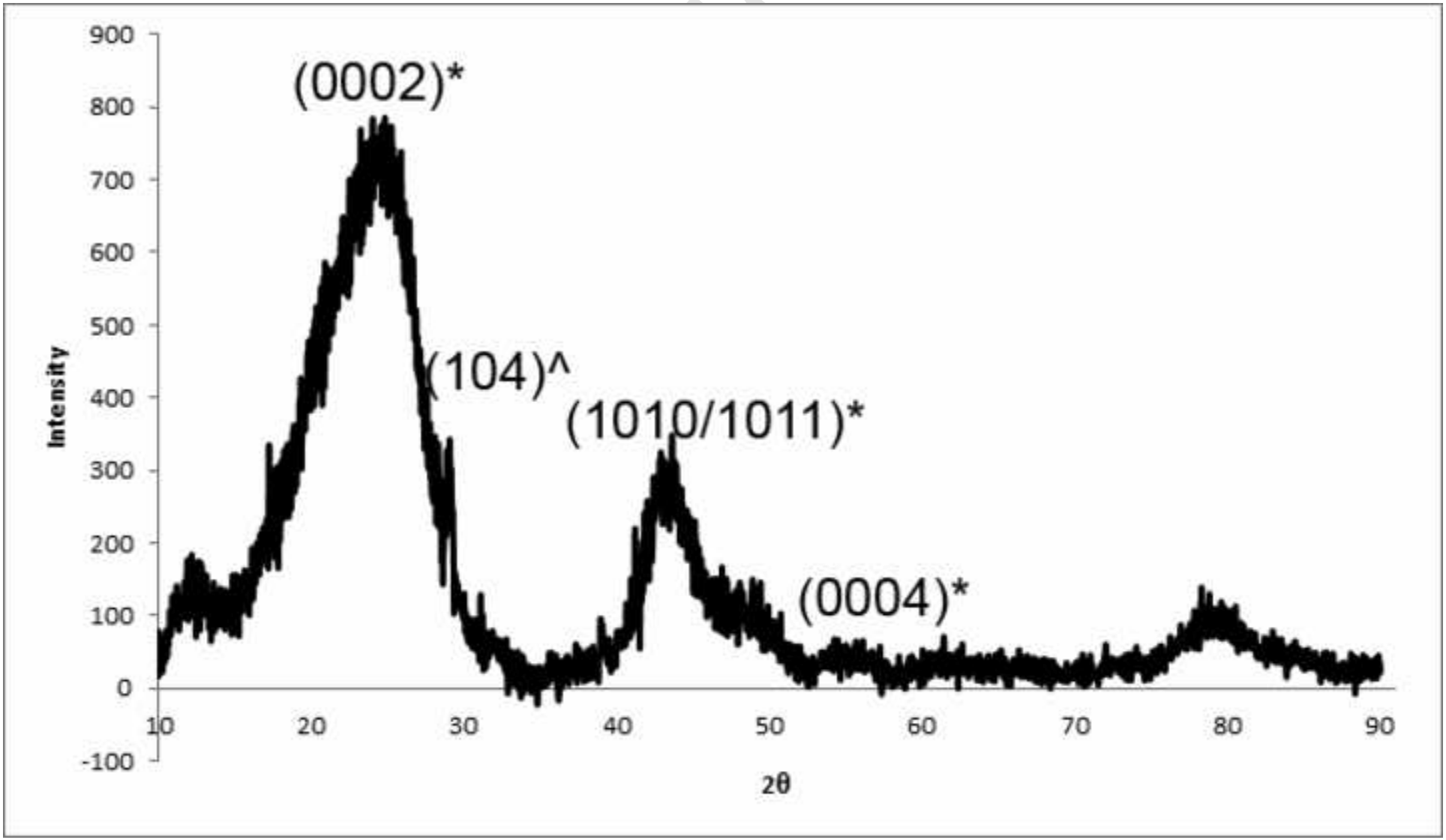
900
800
700
600
500
400
300
200
100
0
-100
Intensity
(0002)*
(104)^
(1010/1011)*
(0004)*
10
20
30
40
50
60
70
80
90
2θ